

Firas Sammoura · JeongJin Kang · Young-Moo Heo
TaeSung Jung · Liwei Lin

Polymeric microneedle fabrication using a microinjection molding technique

Received: 31 August 2005 / Accepted: 20 January 2006 / Published online: 30 May 2006
© Springer-Verlag 2006

Abstract Polymeric microneedles fabricated by microinjection molding techniques have been demonstrated using Topas[®]COC as the molding plastic material. Open-channel microneedles with cross-sectional area of $100\ \mu\text{m} \times 100\ \mu\text{m}$ were designed and fabricated on top of a shank of 4.7 mm in length, 0.6 mm in width, and 0.5 mm in depth. The tip of the microneedle has a round shape with a radius of $125\ \mu\text{m}$ as limited by the drill used in fabricating the mold insert. The injection molding parameters including clamping force, shot size, injection velocity, packing pressure, and temperature were characterized in order to achieve best reproducibility. Experimentally, a fabricated microneedle was successfully injected into a chicken leg and a beef liver freshly bought from a local supermarket and about $0.04\ \mu\text{L}$ of liquid was drawn from these tissues immediately. This new technology allows mass production of microneedles at a low cost for potential biomedical applications.

1 Introduction

Extensive researches have been conducted to provide alternative, and potentially painless needles for trans-

Firas Sammoura and JeongJin Kang have contributed equally to this work

F. Sammoura (✉) · L. Lin
Department of Mechanical Engineering,
University of California, Berkeley, CA 94720, USA
E-mail: firas@me.berkeley.edu
Tel.: +1-510-6428983
Fax: +1-510-6426163

JeongJin Kang · Y.-M. Heo
Korea Institute of Industrial Technology (KITECH),
#401-301, Bucheon TP, 193, Yakdae-dong, Wonmi-gu,
Bucheon-si, Kyunggi-do 420-734, Republic of Korea

TaeSung Jung
JYSolutech, 436-5, Nonhyun-dong, Namdong-gu,
Inchon 405-848, Republic of Korea

dermal drug delivery and blood extraction applications such as insulin delivery for patients with diabetes (Prausnitz 2004; Zahn et al. 2004). The in vivo experiments have shown that microneedles can increase the skin permeability to deliver mixtures of fluids/materials such as peptides, proteins, macromolecules, and vaccines by physically penetrating stratum corneum on epidermis without pain and scar (Martanto et al. 2004).

Previously, microneedles have been fabricated using various kinds of materials, including silicon, metals, and polymers. For example, a combination of surface and bulk-micromachining techniques was used to fabricate microhypodermic needles from a silicon wafer (Lin and Pisano 1999). A hollow metallic microneedle made of palladium has been demonstrated (Brazzle et al. 2000). Microneedles made of parylene have also been presented with enhanced strength (Stupar and Pisano 2001). These and other types of microneedles can be characterized into two groups: (1) in-plane design where the microneedle shank is in the same plane as the substrate (Lin and Pisano 1999; Brazzle et al. 2000; Stupar and Pisano 2001), and (2) out-of-plane design where microneedles are made perpendicular to the substrate (Stoeber and Liepmann 2000). These microneedles have been fabricated based on silicon micromachining processes and the material as well as manufacturing cost might be too high for daily and disposable applications. Alternatively, polymeric material and microinjection molding (Heckele and Schomburg 2004) processes could further reduce the manufacturing cost. This work presents the design, fabrication and testing of in-plane, open-channel microneedles by means of polymeric microinjection molding process toward the goal of mass production of low-cost microneedles.

2 Mold design and fabrication

Figure 1 shows the schematic diagram of the in-plane, open-channel microneedle and Table 1 lists the key dimensions. The key components are the shank portion that has an open-channel on top, and the base portion

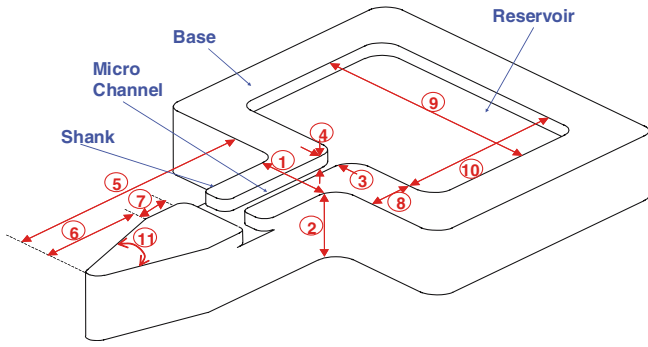


Fig. 1 A schematic diagram of the in-plane, open-channel micro-needle with a liquid reservoir (the micro-needle is not drawn to scale)

Table 1 Key micro-needle design dimensions in Fig. 1

Dimension no.	Value (in.)	Value (μm)
1	0.024 ± 0.001	609.6 ± 25.4
2	0.020 ± 0.001	508 ± 25.4
3	0.004 ± 0.0005	101.6 ± 12.7
4	0.004 ± 0.0005	101.6 ± 12.7
5	0.185 ± 0.001	$4,699 \pm 25.4$
6	0.028 ± 0.001	711.2 ± 25.4
7	0.020 ± 0.001	508 ± 25.4
8	0.080 ± 0.001	$2,032 \pm 25.4$
9	0.400 ± 0.001	$10,160 \pm 25.4$
10	0.400 ± 0.001	$10,160 \pm 25.4$
11	$27.5^\circ \pm 0.1^\circ$	$27.5^\circ \pm 0.1^\circ$

that has a reservoir. The dimension of the micro channel is $100 \mu\text{m}$ in width and $100 \mu\text{m}$ in depth with a total length of 5 mm . The shank is 4.7 mm in length $600 \mu\text{m}$ in width and $500 \mu\text{m}$ in thickness. The tip of the micro-needle has a circular shape with a radius of $125 \mu\text{m}$ as limited by the smallest drill diameter in making the mold insert.

There are only simple guidelines for the design of a runner system in conventional injection molding process. In order to successfully fabricate microneedles by injection molding, special considerations have to be made (Su et al. 2004). The guidelines for traditional injection molding (Menges et al. 2001; Rees 2002) have been adopted as the starting point for the development of a runner system. Figure 2 shows the runner design, which includes a sprue, primary runners, secondary runners and four gates for four cavities.

According to the conventional guidelines, the sprue diameter, D_S , has to satisfy the following condition:

$$D_S \geq D_N + 1.5 \text{ mm}, \tag{1}$$

where D_N is the nozzle diameter of the injection molding machine. On the other hand, the sprue diameter, D_F , has to satisfy the condition below:

$$D_F \geq t_{\text{max}} + 1.0 \text{ mm}, \tag{2}$$

where t_{max} is the maximum thickness of the molded part.

A conventional injection molding machine, FANUC Roboshot α series 30iA was used. The nozzle diameter of the machine is 6 mm and D_S was chosen as 8 mm . The thickness of the micro-needle is about 5 mm as shown in Fig. 1 and D_F was chosen as 8.5 mm . The shape of the

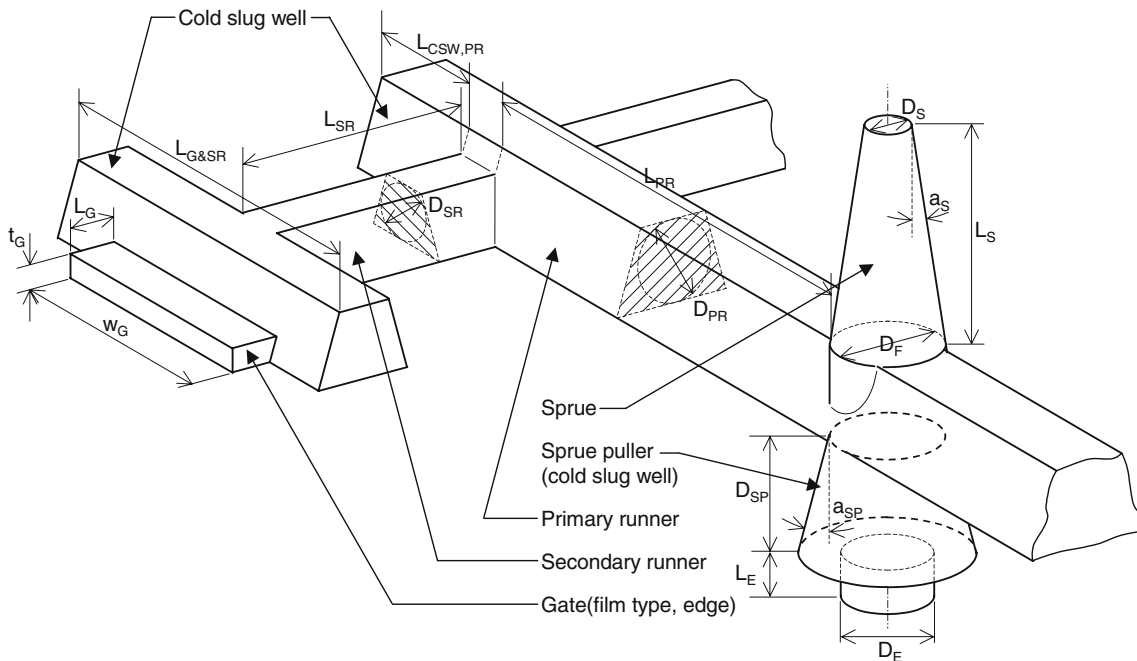


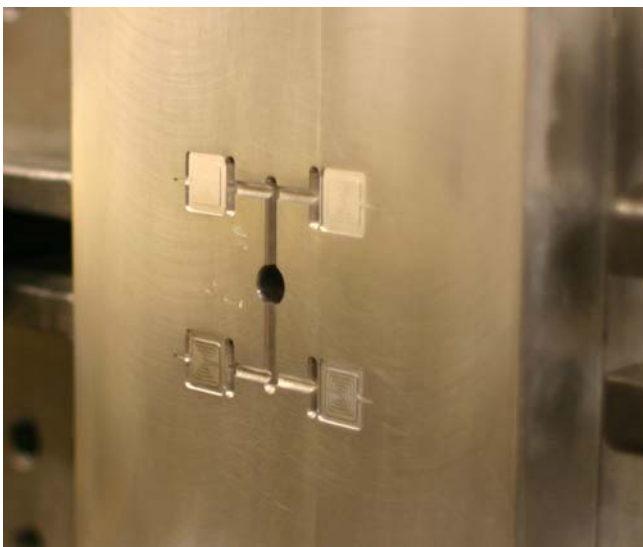
Fig. 2 The schematic of the runner system with the description of main dimensions for the micro-needle fabrication

Table 2 Key runner system design dimensions of Fig. 2

Component	Dimension	Value (mm)
Sprue	D_s	8.00
	D_F	8.50
	L_s	9.53
Primary runner	D_{PR} (semi-circular)	1.98
	L_{PR}	16.5
	$L_{CSW, PR}$	2.24
Secondary runner	D_{SR} (semi-circular)	1.57
	L_{SR}	10.72
	$L_{S, SR}$	12.70
Gate	L_G	0.50
	t_G	0.25
	w_G	10.16

primary and secondary runners is selected to be a semi-circular type (instead of the trapezoidal shape as shown Fig. 2) such that a molded set can be easily released from the fixed half of the mold insert. The primary and secondary sprue runners were machined using ball milling with the mill radii of 1.98 mm (0.078 in.) and 1.57 mm (0.062 in.), respectively. Conventionally, the thickness of the gate is usually about 50–60% of maximum thickness of the molded part, whereas its length is usually 0.5 mm and its width is chosen to be the same as the edge width of the molded component. A film gate (edge gate) was selected and its thickness was set as 250 μm following the guidelines of 50–60% of the maximum thickness of the molded part. Table 2 lists the detailed dimensions of the runner system of Fig. 2.

Figure 3 shows a digital picture of the aluminum mold insert that was machined by using precision NC machining and the smallest drill used in the process has a diameter of 250 μm (0.01 in.). Mold insert surfaces through which plastic resin goes were machined to be very smooth (63 $\mu\text{in.}$ surface finish) in order to prevent sticking of plastic materials.

**Fig. 3** A digital photo of the aluminum mold insert fabricated by precision machining

3 Microneedle fabrication

Topas[®] COC from Ticona Inc. (Ticona North American Headquarters, 8040 Dixie Highway, Florence, KY 41042, USA) was used in the prototype process and processing parameters such as temperature, injection speed, pressure, clamping force, and decompression velocity have been characterized to optimize the molding results. The temperature was set at 230°C in order to maintain the plastic material in the molten state. The clamping force was set at 30 metric tons and the maximum injection pressure was set at 17,000 psi—both of these parameters are near the maximum capacity of the Roboshot α -30i_A. The shot size of 0.4 in. was selected, as beyond which flush will occur. The cooling time is set at 90 s to ensure that the molded pieces have fully solidified. A two-stage packing sequence was chosen, each cycle with duration of 5 s, the first of which was set at 2,000 psi and the second at 3,000 psi. A graphite-based dry mold release (Graphite Plus from Asbury Carbons Inc., 405 Old Main Street, P.O. Box 144, Asbury, NJ 08802, USA) has been used to enhance the releasing step of the molded part. Figure 4a is a digital photo of the fabricated microneedle along side a US coin of a dime. The surface of the microneedle seems to be rough from this prototype fabrication result while the shape of the reservoir can be clearly identified. Figure 4b is the top view SEM micrograph of the microneedle. The width of the open-channel is 100 μm as defined by the distance of two drilling steps on the mold insert using a drill of 250 μm in diameter to define the two supporting side-edges as shown. Figure 4c is a close-up view showing the microneedle tip region. The tapered bottom surface at the top of the T-shape channel can be observed as the result of the mold insert manufacturing process. The T-shape channel design is to keep the sharp and solid tip of the microneedle for easy penetration of tissues while liquid could be delivered/extracted from both openings of the T-shape channel.

4 Testing and discussions

The injection molding system with the designed mold insert has been simulated using *Moldflow* [Moldflow Corporation, MPI (Moldflow Plastics Insight), version 5.0]. The required maximum injection pressure for a specific injection fill time was simulated as shown in Fig. 5. It is observed that under a maximum injection pressure of 17,000 psi (117 MPa), filling of the mold cavities is theoretically completed as long as the fill time is less than 2.5 s. Experimentally, the injection speed was varied with 0.2, 0.5, 1, and 2 in./s and the filling time is defined as:

$$\text{Filling_time} = \frac{\text{shot_size}}{\text{injection_speed}} \quad (3)$$

Therefore, the filling times for these experiments are 2, 0.8, 0.4, and 0.2 s, respectively, and Fig. 6 shows the

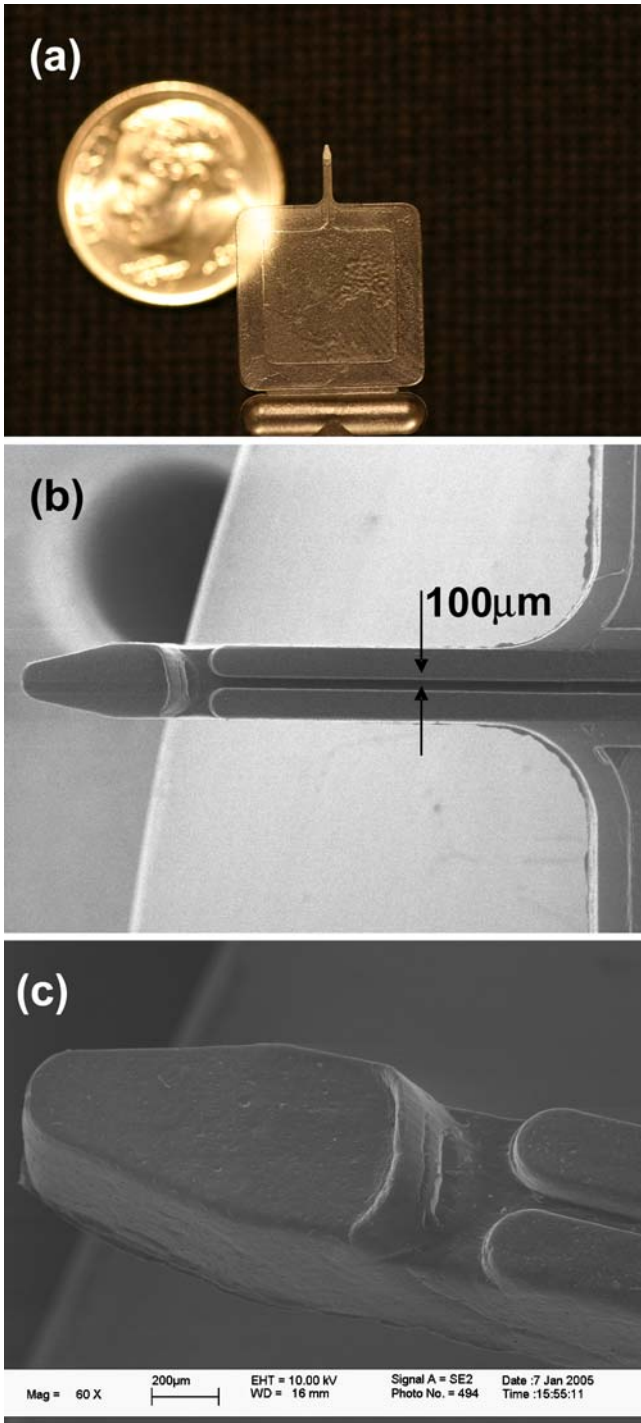


Fig. 4 **a** A digital photo of a molded microneedle and the background is an US coin of a dime, **b** top view SEM micrograph of the microneedle with an open-channel design and the width of the T-shape channel is 100 μm , and **c** a close-up SEM micrograph showing the tip region

fabrication results. It is observed that insufficient filling occurs in Fig. 6a and b when the filling times are 2 and 0.8 s and this contradicts the simulation result. Several issues could contribute this discrepancy during the microinjection molding process: (1) roughness of the

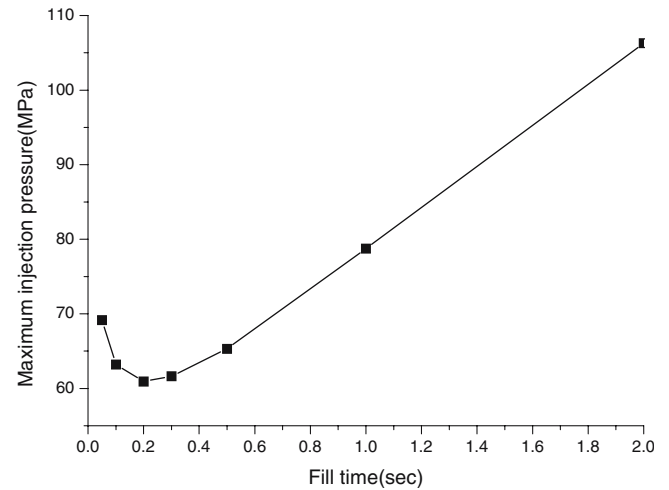


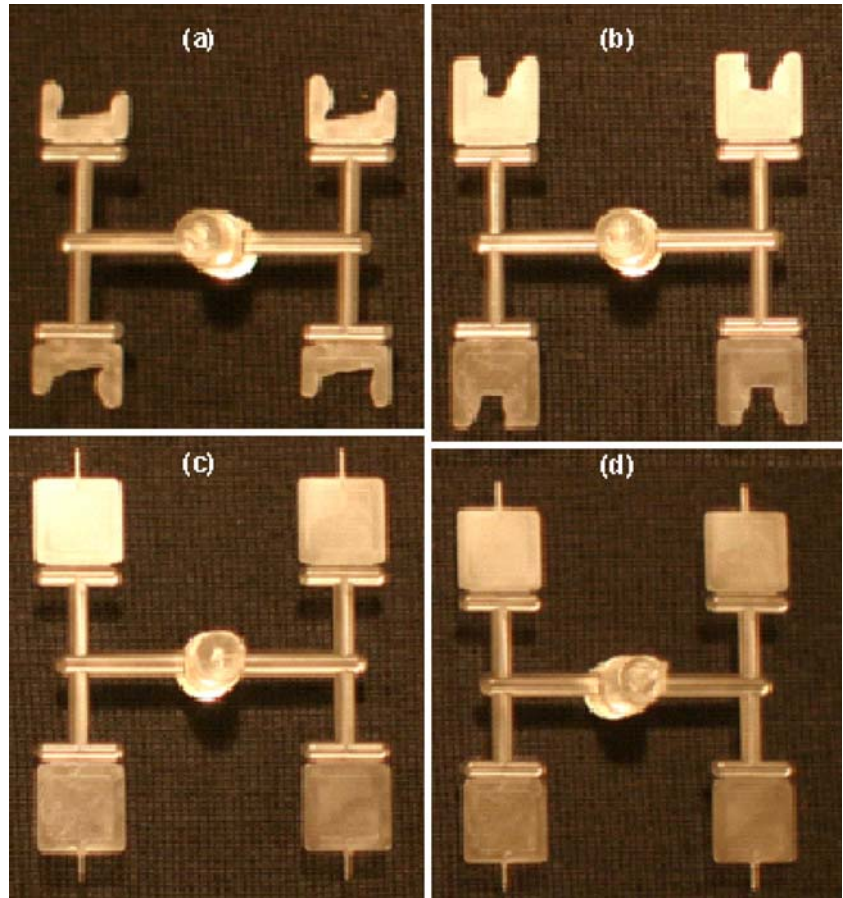
Fig. 5 Simulation data showing the maximum injection pressure versus filling time

mold surfaces could play a more dominant role during the molding process and was not accounted for in the simulation, (2) changes in dimensions between the mold insert as drawn and the mold insert as fabricated, and probably the most important one (3) the mold cavity temperature was assumed to be 55°C in the simulation whereas in reality that value was not controlled in the experiments. Further studies are needed to investigate this discrepancy with more experiments and possibly new simulation algorithms.

Table 3 lists the measured dimensions of two fabricated samples as compared with the design values. The lateral dimensions were measured under a microscope and the error bars were estimated values due to the variations of the molded geometries. The thickness measurement is done by using a micrometer and the estimation of error is 25 μm . These two samples are from two different sites of the microneedle set such that dimensional differences are expected. It is observed that all lateral dimensions fall within the design values except part#5 of sample 1. We observed that this particular sample was bent before the measurement due to repeated penetration tests and this causes the reduction of length measurement under the optical microscope. On the other hand, the thickness measurements show about 100 μm more than the design value. One possible reason is the tightness of the seal of the mold insert.

In order to test the capability of the microneedle in penetrating tissues and aspirating/injecting fluids, a fresh chicken leg and a beef liver were bought from a local supermarket. Figure 7 shows that the microneedle was capable of penetrating the chicken leg. It was observed that the skin of the chicken was bent inwards during the process while the microneedle maintained its shape. Figure 8 shows the beef liver test under an optical microscope. It is observed that liquid immediately spread out into the microchannel and the liquid front stops as illustrated in Fig. 8. The total movement of the

Fig. 6 Fabricated microneedle sets with different filling time. **a** 2.0 s, **b** 0.8 s, **c** 0.4 s, and **d** 0.2 s



liquid front is about 350 μm and the total liquid volume is about 0.04 μL .

5 Conclusion

We have demonstrated an in-plane, open-channel microneedle fabrication using plastic injection molding. The fabricated plastic microneedles were compared with the design values and good reproduction results were achieved. Simulation of the injection system was carried out using Moldflow and the relation between maximum injection pressures and filling times were analyzed. The range of filling time over which the mold cavities are completely filled as predicated in theory was compared to actual injection molding data. Discrepancy between

Table 3 Measured and design dimensions

Dimension of part no.	Sample 1 (μm)	Sample 2 (μm)	Design Value(μm)
1	619 \pm 15	609.5 \pm 15	609.6 \pm 25.4
2	596.9 \pm 25	594.4 \pm 25	508 \pm 25.4
3	97.5 \pm 10	92 \pm 10	101.6 \pm 12.7
5	4,530 \pm 50	4,698.5 \pm 50	4,699 \pm 25.4
6	729 \pm 15	702 \pm 15	711.2 \pm 25.4
11	30° \pm 2°	24° \pm 2°	27.5° \pm 0.1°

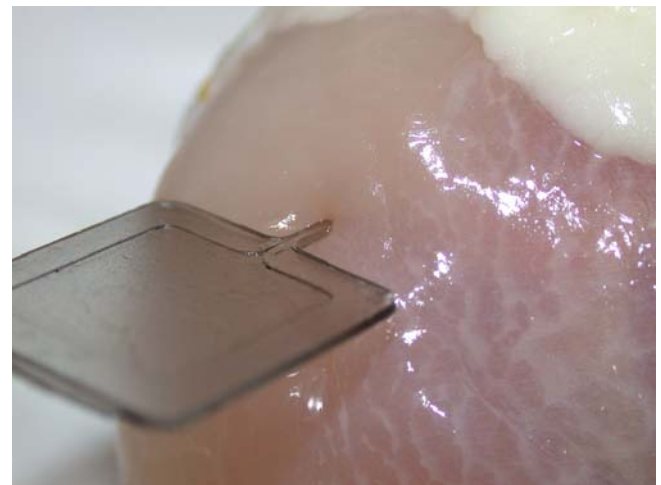


Fig. 7 A microneedle is inserted in a chicken leg

experiments and simulation results were found. Although mold insert temperature control is identified as the major reason for the discrepancy, further investigations are required. Experimentally, microneedles were able to penetrate fresh chicken leg and beef liver and fluids were observed to be drawn out into the micro-channel immediately

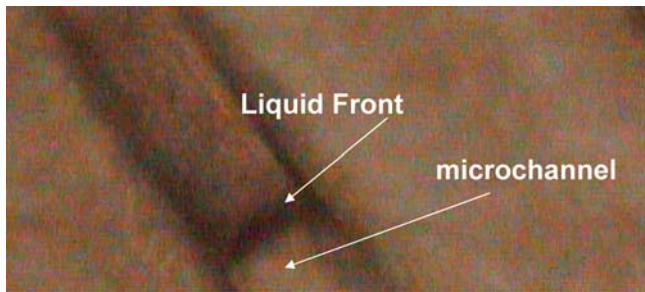


Fig. 8 Liquid front in the microneedle channel coming out of a beef liver

Acknowledgements This project is supported in part by a grant from Korea Institute of Industrial Technology and an NSF award DMI0428884. The mold insert was fabricated in the UC-Berkeley Mechanical Engineering Machine Shop with the assistance of Mr. John Morton and the authors would like to thank Mr. Ron Wilson for taking SEM pictures.

References

- Brazzle D, Bartholomeusz R, Davies J, Andrade J, Van Wageman RA, and Frazier AB (2000) Active microneedles with integrated functionality. In: Proceedings of solid state sensor and actuator workshop, Hilton Head, pp 199–202
- Heckele M, Schomburg WK (2004) Review on micro molding of thermoplastic polymers. *J Micromech Microeng* 14:R1–R14
- Lin L, Pisano AP (1999) Silicon-processed microneedles. *IEEE J Microelectromech Syst* 8:178–184
- Martanto W, Davis SP, Holiday NR, Wang J, Gill HS, Prausnitz MR (2004) Transdermal delivery of insulin using microneedles in vivo. *Pharm Res* 21:6947–6952
- Menges G, Michaeli W, Mohren P (2001) How to make injection molds, 3rd edn. Carl Hanser Verlag, Munich, Germany
- Prausnitz MR (2004) Microneedles for transdermal drug delivery. *Adv Drug Deliv Rev* 56:581–587
- Rees H (2002) Mold engineering, 2nd edn. Carl Hanser Verlag, Munich, Germany
- Stoeber B, Liepmann D (2000) Fluid injection through out-of-place microneedles. In: 1st annual international IEEE-EMBS special topic conference on microtechnologies in medicine and biology, Lyon, France, pp 224–228
- Stupar PA, Pisano AP (2001) Silicon, parylene, and silicon/parylene microneedles for strength and toughness. In: Proceedings of the 11th international conference on solid-state sensors and actuators (Transducers '01), Munich, Germany
- Su YC, Shah J, Lin L (2004) Implementation and analysis of polymeric microstructure replication by micro injection molding. *J Micromech Microeng* 14:3415–3422
- Zahn JD, Deshmukh A, Pisano AP, Liepmann D (2004) Continuous on-chip micropumping for microneedle enhanced drug delivery. *Biomed Microdevices* 6:183–190